

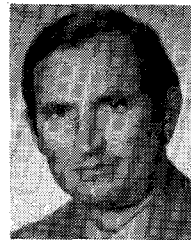
- [23] D. Poulin, "Load-pull measurements," *Microwaves*, pp. 61-65, Nov. 1980.
- [24] J. P. R. David, J. E. Sitch, and M. S. Stern, "Gate-drain avalanche breakdown in GaAs power MESFET's," *IEEE Trans. Electron Devices*, vol. ED-29, pp. 1548-1552, Oct. 1982.



Andrzej Materka was born in Łęczyca, Poland, on November 18, 1949. He received the M.Sc. degree in radio engineering from Warsaw Technical University and the Ph.D. degree in technical sciences from Łódź Technical University, in 1972 and 1979, respectively.

From 1972 to 1974, he worked for the Radio and Television Broadcasting Stations, Łódź, on transmitters and circuits for space division of video signals. Later, he joined the Institute of Electronics, Łódź Technical University, to serve as a Research and Teaching Assistant on testability of analog circuits, CAD design, and semiconductor devices modeling. Since 1979, he has been a Lecturer at the same university. From 1980 to 1982, he was with the Research Institute of Electronics, Shizuoka University, Hamamatsu, Japan, where he worked on microwave power combining techniques and

FET oscillators design. His current research interests include semiconductor devices modeling, CAD design, and medical electronics.



Tomasz Kacprzak was born in Vienna, Austria, on April 27, 1945. He received the M.Sc. degree in electronics engineering from Warsaw Technical University and the Ph.D. degree in technical sciences from Łódź Technical University, in 1969 and 1977, respectively.

From 1969 to 1970, he worked for the Wrocław Electronic Factory, Wrocław, Poland, on electronic circuits for ferrite core computer memory. Later, he joined the Institute of Electronics, Łódź Technical University, to serve as a Research As-

sistant on semiconductor devices modeling and CAD design. Since 1977, he has been a Lecturer at the same university. From 1980 to 1981, he spent six months at the Institute of Circuit Theory and Telecommunications, Technical University of Denmark, Lyngby, Denmark as a Research-Scholarship Holder, where he worked on modeling of MOS transistors. His current research interests include analysis of nonlinear distortions in electronic analog circuits, semiconductor devices modeling, and CAD design.

Dr. Kacprzak is a member of the Polish Society of Theoretical and Applied Electrical Science (PTETIS).

Short Millimeter Wavelength Mixer with Low Local Oscillator Power

WILLIAM HANT, SENIOR MEMBER, IEEE

Abstract — This paper discusses development, for the 240-GHz region, of whisker contacted diode mixers with LO powers between 10 and 50 μ W. Mixer requirements for low parasitic diodes, situated in high-embedding impedance circuits are described and appropriate RF and IF circuit designs presented. A capacitive post RF matching circuit for a full-height waveguide is developed with superior bandwidth characteristics at high impedance levels and greater ease of fabrication than usual matching circuits in reduced height guide. Corroborating experimental results are presented for an X-band model and for a 235-GHz mixer.

I. INTRODUCTION

THE BEST MIXER performance within the 240-GHz region has been accomplished using whisker contacted Schottky barrier diodes situated in waveguide structures. The 1-10-mW LO power typically required for these fundamental mixers has usually been supplied by millimeter-wave tubes and more recently by a frequency tripled whisker contacted Gunn oscillator¹ with 2-mW output.

Reduction of the LO power requirements to levels achievable with monolithic planar solid-state sources would simplify the system design and enhance the practicality of these mixers for tactical applications. This paper discusses the development of high-impedance room-temperature Schottky diode mixers with LO powers typically between 10 and 50 μ W. Included in the paper are a) the analysis of the mixer under low LO power operation, b) the use of a novel capacitive stub impedance transformer to provide a high-embedding impedance diode mount in full-height waveguide, and c) experimental results for both an X-band simulating model and for a mixer operated at 235 GHz.

II. DIODE AND CIRCUIT REQUIREMENTS FOR LOW LO POWERS

The operation of mixer diodes at low LO power is conceptually no different than a mixer operating with the usual LO drive. In order to get efficient mixing, the LO voltage must be adequate to sweep the diode over a wide range of differential resistances. For millimeter-wave mixer diodes operating typically with \sim 1-mW LO drive, this

Manuscript received February 9, 1984; revised August 28, 1984.

The author is with Northrop Research and Technology Center, One Research Park, Palos Verdes Peninsula, CA 90274.

¹The 0.5-dB insertion loss was measured with a fixed 750- Ω resistor in place of the diode. This resistance is an average of diode resistance measurements taken previously without the IF matching circuit.

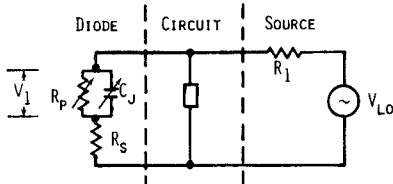


Fig. 1. Simplified diagram for the mixer LO circuit.

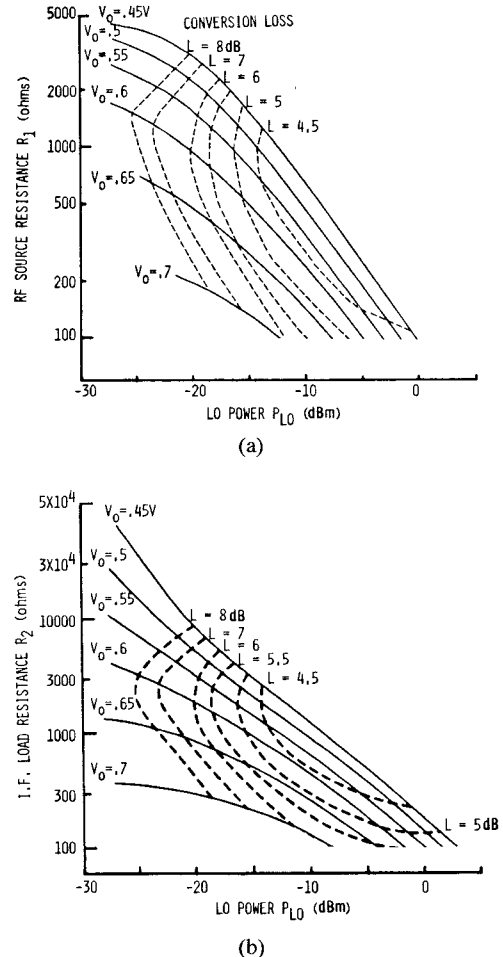
voltage sweeps the diode over the required range in the vicinity of $\sim 50 \Omega$. In order to achieve efficient mixing with low LO drive, one must adjust the diode bias so that the differential diode resistance is much greater than 50Ω . This paper describes the operation of a diode mixer at high impedances and the circuits necessary to match the incoming RF signal to the diode and the output IF signal to a conventional IF amplifier at $\sim 50 \Omega$.

For operation at high impedances, one must pay particular attention to the parasitic impedances of the diode in order to prevent loss of efficiency due to both LO power and signal power being absorbed or reflected there. Consider the simplified mixer LO equivalent circuit shown in Fig. 1 and assume sinusoidal LO voltage excitation. The diode is represented by nonlinear resistance R_p , by nonlinear junction capacitance C_j , and by series resistance R_s . The LO voltage V_1 across the diode must exceed a minimum value so that the mixer diode is in a sufficiently nonlinear region where the RF signal input power is efficiently converted to the IF output. Under ideal conditions with no parasitics ($C_j, R_s = 0$), the required V_1 could be achieved at very low LO power by making R_p very large. With parasitics, part of the LO power incident on the diode is diverted by C_j and dissipated by R_s . The relationship between P_{LO} the power absorbed by the diode, P_{RP} the modulation power required by R_p , and P_{RS} the power wasted by R_s is given by

$$P_{LO} = P_{RP} + P_{RS} \quad (1)$$

where $P_{RP} = V_1^2/2R_p$, $P_{RS} = 0.5V_1^2R_s(R_p^{-2} + \omega_{LO}^2C_j^2)$, ω_{LO} = LO frequency. Note that since the lower limit for V_1 is fixed by the diode nonlinear conversion characteristics, power loss P_{RS} for high R_p is controlled by $\omega_{LO}^2C_j^2R_s$. The quantity $\omega_{LO}^2C_j^2R_s$ is thus a useful figure of merit, dependent on LO frequency and diode parasitics, that should be minimized for the diode selection of low LO power mixers.

A computer analysis was performed to determine the required diode embedding impedances and bias conditions necessary for minimizing conversion loss at low LO power levels. The analysis assumes wide-band single-ended Y mixers with exponential diodes and uses well-known expressions for the RF and IF circuits such as given by Saleh [2] and McColl [3]. An expression for the effective value of C_j given as a function of V_1 and the bias voltage is derived in the Appendix. In order to obtain realistic estimates of the LO power requirements, we chose characteristics of commercially available low-parasitic Schottky barrier diodes. Calculations were performed for $f_{LO} = 235$ GHz using the manufacturer supplied specifications of $R_s = 10 \Omega$, $C_{j0} = 2 \times 10^{-15} \text{ F}$ for 1- μm -diam Millimeter Wave Tech-

Fig. 2. (a) Diode RF source resistance R_1 and (b) IF load resistance R_2 versus LO power for constant bias voltages ($C_{j0} = 2 \times 10^{-15} \text{ F}$, $R_s = 10 \Omega$, $f_{LO} = 235 \text{ GHz}$).

nology SD017 diodes. It was assumed that the RF source resistance R_1 matches the diode at the LO frequency and that the IF load resistance R_2 matches it at the IF. Fig. 2(a) shows the relationship between R_1 and LO power calculated for different bias voltages.

The optimum operating conditions for fixed LO powers are obtained by means of the contour lines for constant conversion loss. For example, given an available LO power P_{LO} of -20 dBm ($10 \mu\text{W}$), Fig. 2(a) indicates that the lowest conversion loss L of 5.9 dB occurs for $R_1 \approx 950 \Omega$ at bias voltage $V_0 = 0.6 \text{ V}$. For $P_{LO} = -14 \text{ dBm}$, the lowest conversion loss of 4.5 dB occurs for $R_1 \approx 800 \Omega$. The corresponding matching resistance R_2 for the IF circuit obtained from Fig. 2(b) are 1200 and 1000Ω , respectively. The above results show that mixers built with low-parasitic diodes are capable of good conversion loss at low LO powers, provided that the diodes are situated in RF and IF circuits of appropriately high-embedding impedances.

III. DESIGN OF HIGH-IMPEDANCE CIRCUITS

Matching of the mixer diode to the waveguide at the signal and LO frequencies was accomplished by means of a capacitive post matching scheme that is well suited for high impedances. Fig. 3(a) shows a waveguide cross-sectional

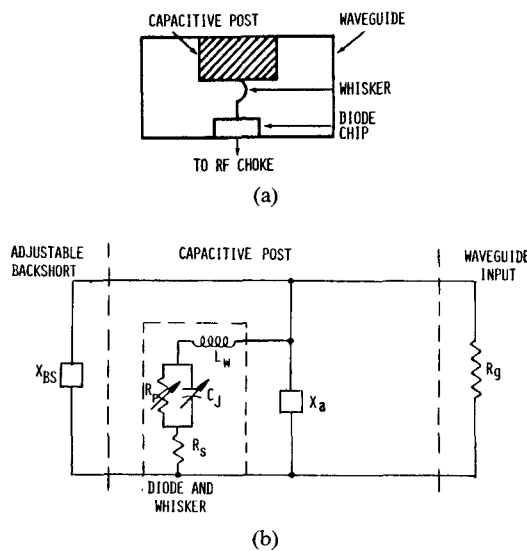
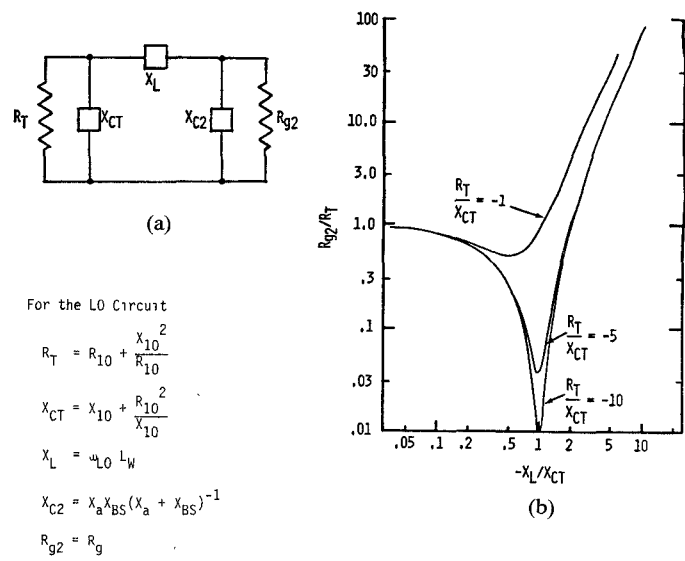


Fig. 3. RF matching circuit for the 235-GHz mixer. (a) Sectional view of waveguide. (b) Equivalent circuit at LO frequency.

view of the diode and RF matching network. The bottom surface of the diode chip is attached to a microstrip RF choke circuit that reflects the RF signals and passes the IF. The top surface contains a large array of Schottky barrier diodes. Contact to one of the diodes occurs by means of a bent whisker whose tip has been etched to the diode diameter. The other whisker end is attached to a circular cylindrical capacitive post that is centered on the broad-wall of the waveguide. RF power at the signal and LO frequencies is incident on the mixer from one end of the full-height waveguide. The other end is terminated by a variable backshort that is used for tuning the mixer. An important feature of this circuit is the broad-band behavior of the capacitive post. Because of its close proximity to the diode, the post is an effective and wide-band matching element that tunes out reactances caused by the diode parasitics and whisker inductance. In addition, this full-height waveguide mixer is easier to fabricate than typical millimeter-wave mixers situated in a reduced height guide [4] because it eliminates the need for a waveguide transformer and utilizes a larger backshort.

Electrical design of the RF matching circuit was performed by means of the equivalent circuit shown in Fig. 3(b). Circuit elements referred to the diode centerline were obtained in the following manner. Using measurements of the diode $I-V$ characteristics and zero-bias capacitance as input conditions for the mixer analysis program, we determined the circuit source resistance R_1 and diode parameters R_p , C_j , and R_s necessary for low LO power operation. Inductance L_w of the whisker was calculated by means of an approximate formula, given by Sharpless [5], for a thin wire situated at the center of the waveguide.

The capacitive post was represented as follows. Typically, the equivalent circuit for the driving point impedance at the bottom of a post in a waveguide consists of a reactance to represent the gap, in series with an inductive reactance to represent the post. The analysis by Eisenhart



$$\text{For the LO Circuit}$$

$$R_T = R_{10} + \frac{X_{10}^2}{R_{10}}$$

$$X_{CT} = X_{10} + \frac{R_{10}^2}{X_{10}}$$

$$X_L = \omega_{LO} L_w$$

$$X_{C2} = X_a X_{BS} (X_a + X_{BS})^{-1}$$

$$R_{g2} = R_g$$

$$\text{where } R_{10} = [(R_p + R_s) + R_s R_p^2 \omega_{LO}^2 C_j^2] (1 + \omega_{LO}^2 C_j^2 R_p^2)^{-1}$$

$$X_{10} = -\omega_{LO} C_j R_p (1 + \omega_{LO}^2 C_j^2 R_p^2)^{-1}$$

Fig. 4. Matching circuit and conditions for match. (a) Equivalent circuit. (b) R_{g2}/R_T versus X_L/X_{CT} .

and Khan [6] suitable for thin posts with post diameter to waveguide width ratio $d/a < 0.14$ indicates that the inductive reactance of the post decreases as d/a increases. Based on these results, we assume that, for the large post diameter to waveguide width ratio ($d/a \approx 0.4$) used in this design, the inductive post reactance is small compared to the gap reactance. The equivalent circuit is thus approximated by a single gap reactance. The gap reactance is interpolated from experimental results of post reactances in waveguide given by Marcuvitz [7]. Marcuvitz represents the post by a T network consisting of reactance X_a and two equal reactances X_b that are in series with the equivalent impedances contributed from both sides of the waveguide circuits. The millimeter-wave mixer is designed with post height to waveguide height ratio $l/b = 0.45$ for which the reactance to waveguide impedance ratio X_b/R_g is small and $X_a/R_g = -0.55$ is approximately constant over the center of the waveguide band. For these conditions, the capacitive post can be approximated by reactance X_a .

In order to ascertain the relative importance of the different circuit elements in effecting the match, consider the reduced equivalent-circuit diagram shown in Fig. 4(a). Here the diode elements R_p , C_j , R_s , and the whisker inductance L_w of Fig. 3(b) are replaced by diode equivalent resistance R_T , by diode capacitive reactance X_{CT} , and by whisker inductive reactance X_L . Note also that for a perfect match and with no assumed circuit loss, $R_T = R_1$. The remaining impedances in Fig. 3(a) consisting of the mount and backshort reactances X_a and X_{BS} and waveguide impedance R_g are replaced in Fig. 4(a) by reactance X_{C2} in parallel with resistance R_{g2} .

To determine how the circuit of Fig. 4(a) is to be matched, consider which circuit elements are variable. Since R_T and X_{CT} are functions of the diode characteristics, they

are fixed. Also, for a given LO frequency, R_{g2} is fixed. The match is accomplished by adjusting the whisker length to change X_L and the capacitive post dimensions and variable backshort location to change X_{C2} . A design goal for achieving an optimum LO tuning bandwidth is to choose the dimensions of the whisker and capacitive post so that the backshort is a quarter guide wavelength from the diode and $X_{BS} \rightarrow \infty$. Design curves to determine the circuit values required for a match are given in Fig. 4(b).

The purpose of the IF matching network is to transform the 50Ω input resistance of the IF amplifier to R_2 , the mixer output resistance. In parallel with R_2 is an equivalent capacitive reactance due to the RF choke which also must be considered in the matching. We can use a π matching circuit for the IF impedance transformation as was done for the RF match. Using the circuit shown in Fig. 4, we let R_T represent the diode resistance R_2 and R_{g2} represent the input resistance of the IF amplifier. Reactance X_{CT} represents the parallel combination consisting of two capacitive reactances. One reactance is for the RF choke and the other for a capacitor C_1 that is added to the circuit to optimize bandwidth. Reactance X_L represents inductance L_1 of the IF circuit. Reactance X_{C2} is needed to complete the impedance match. The bandwidth of the IF matching circuit typically exceeds 40 percent. The circuit was implemented on quartz substrate by means of hybrid integrated-circuit elements [8].

IV. MIXER EVALUATION

Because of mixer fabrication problems and difficulties in instrumentation at 235 GHz, much of the experimental evaluation was performed on an *X*-band model. Despite slightly higher parasitics, the *X*-band model simulates most of the important features of the 235-GHz device. These features include high-embedding impedance, the same full-height RF matching scheme with a capacitive matching post, and similar RF choke and IF matching networks using microstrip and hybrid integrated circuits. For the model mixer shown in Fig. 5(a), a small packaged diode and pin replace the diode chip and whisker of the 235-GHz mixer shown in Fig. 3(a). The additional diode package capacitance and pin inductance do not significantly effect bandwidth and can be compensated for by the capacitive post and the backshort. Circuit parameters, conversion loss, and bandwidths calculated for $P_{LO} = 10 \mu\text{W}$ are compared in Table I for the 235-GHz and *X*-band model mixers. Results indicate that conversion loss is quite comparable and the figure of merit $\omega_{LO}^2 C_j^2 R_s$ is slightly worse for the *X*-band model. Note also the difference in effective diode resistance to capacitive reactance ratio R_T/X_{CT} for the two devices. This difference occurs primarily because of the diode parameters and accounts for the larger RF bandwidth of the 235-GHz mixer. The IF circuit for the 235-GHz device was frequency scaled from the *X*-band model circuit that matches to $R_2 = 770 \Omega$. The scaled circuit is thus mismatched to $R_2 = 1200 \Omega$ required by the

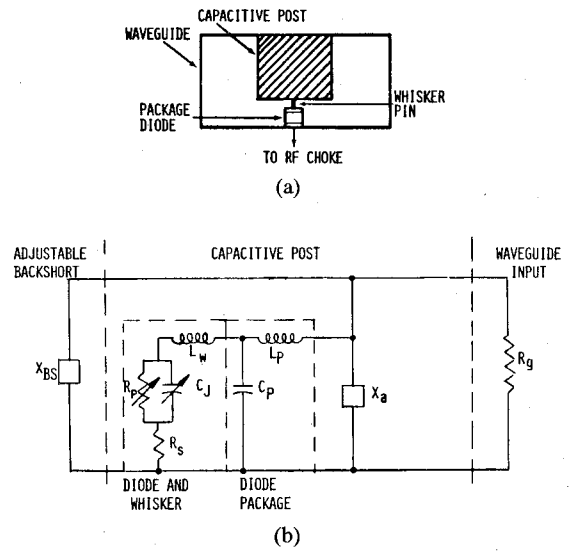


Fig. 5. RF matching circuit for the *X*-band model mixer. (a) Sectional view of waveguide. (b) Equivalent circuit at LO frequency.

TABLE I
COMPARISON OF CALCULATED CHARACTERISTICS FOR THE 235 GHz
AND *X*-BAND MODEL MIXERS FOR $P_{LO} = 10 \mu\text{W}$

| Parameters | 235 GHz Device (Millimeter Wave Technology SD017 Diode) | <i>X</i> -Band Model (9.96 GHz) (Alpha 6600 Diode) |
|--|---|---|
| LO Power (dBm) | -20 | -20 |
| LO frequency f_{LO} (GHz) | 235 | 9.96 |
| Bias Voltage (V) | 0.6 | 0.55 |
| Figure of Merit $\omega_{LO}^2 C_j^2 R_s$ | 3.5×10^{-4} | 7.9×10^{-4} |
| LO frequency Circuit Reactances (Ω) | $X_{CT} = -172$ $X_L = 275$ $X_{C2} = -118$ | $X_{CT} = -35.6$ $X_L = 75.3$ $X_{C2} = -39.9$ |
| Diode Impedance Ratio R_T/X_{CT} (Figure 4) | -5.29 | -13.5 |
| Conversion Loss (dB) | 5.9 | 6.3 |
| 3dB RF Bandwidth (%) | 19 | 4 |
| I.F. frequency (MHz) | 750 | 30 |
| Diode I.F. Resistance R_2 (Ω) | 1200 | 770 |
| 3dB I.F. Bandwidth (%) | 43 | 54 |
| I.F. Circuit Reactances (Ω) | $X_{CHOKE} = -1061$ $X_{C1} = -241$ $X_{L1} = 188$ $X_{C2} = -196$ | $X_{CHOKE} = -1061$ $X_{C1} = -241$ $X_{L1} = 188$ $X_{C2} = -196$ |

235-GHz device, and as a consequence has slightly narrower IF bandwidth than the model mixer.

V. *X*-BAND MODEL MIXER

The *X*-band model mixer, shown schematically in Fig. 6, consists of two parts: a printed circuit part that includes the RF choke, IF matching network, and bias feed, and a waveguide part that contains the backshort, capacitive

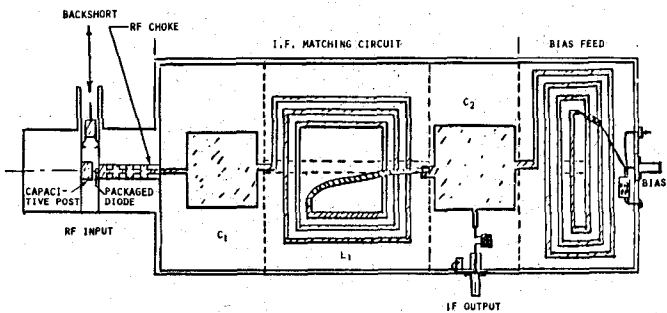


Fig. 6. Schematic for the X-band model mixer.

TABLE II
SUMMARY OF DIMENSIONS AND DIODE PARAMETERS FOR THE
MIXER EXPERIMENTS

| | X-Band Model (9.96 GHz) | 235 GHz Device |
|-----------------|---|--|
| Waveguide | Height $b = .400$ in. Width $a = .900$ in. | $b = .0215$ in. $a = .043$ in. |
| Capacitive Post | Diameter $d = .360$ in. Length $l = .245$ in. | $d = .0172$ in. $l = .0097$ in. |
| Whisker | Straight pin $d = .013$ in; $l = .050$ in | Bent AuNi wire $d = .001$ in. |
| RF Choke | 4 52 Ω sections .220 X .150 in. 3 110 Ω sections .044 X .134 in. .117 in. quartz substrate | 4 52 Ω sections .009 X .0064 in. 3 110 Ω sections .0019 X .0057 in. .005 in. quartz substrate |
| Diode | Alpha 6600 Package $d = .085$ in. $l = .105$ in. | Millimeter Wave Technology SD017 Chip .010 X .010 X .004 in (1 micron diodes) |
| | Measured Diode Parameters $i_{sat} = 1.81 \times 10^{-14} A$; $R_s = 1.72$ $C_{j0} = 9.2 \times 10^{-14} F$ n (ideality) = 1.22 | Measured Diode Parameters $i_{sat} = 8.39 \times 10^{-17} A$ $R_s = 14.8 \Omega$ $C_{j0} = 4 \times 10^{-15} F$ (with LO power) $n = 1.33$ |

post, and the pin-contacted packaged diode. The RF choke was fabricated on quartz microstrip and utilizes four quarter-wave sections of 110 Ω and 52 Ω impedance. Measured insertion loss was greater than 30 dB over the LO tuning bandwidth of the mixer. Details of the circuit dimensions and diode parameters are given in Table II.

The IF matching circuit, consisting of hybrid circuit capacitances C_1 , C_2 and inductance L_1 , was fabricated on a quartz substrate using copper tape applied to both surfaces of the quartz. Physical location of the components and the circuit shielding were empirically adjusted to yield a minimum insertion loss of less than 0.5 dB¹ and an IF bandwidth of 45 percent.

The RF match to the diode was obtained semi-empirically by optimizing length l of the whisker pin. From waveguide admittance measurements taken for a circuit with dimensions obtained from the theoretical model² of Fig. 5, we noted that the diode was initially matched near $f = 11.0$ GHz. This match was then shifted toward the waveguide band center near $f = 10.1$ GHz by increasing l from 0.026 to 0.045 in. The resulting measured admittance for different frequencies is shown in the Smith Chart plot of Fig. 7 for backshort positions of optimum match and for infinite

²For the model mixer $l/b = 0.61$. Based on Marcuvitz's results, the representation of the capacitive post by X_a for this case may be less accurate than for the millimeter-wave mixer with $l/b = 0.45$.

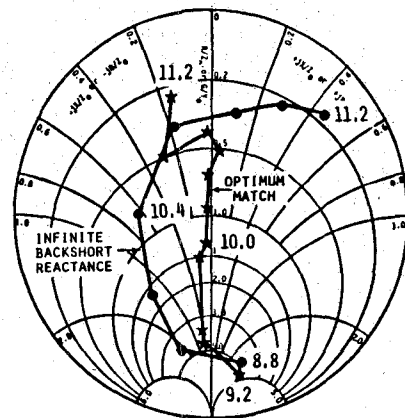


Fig. 7. Measured admittance for the X-band model mixer.

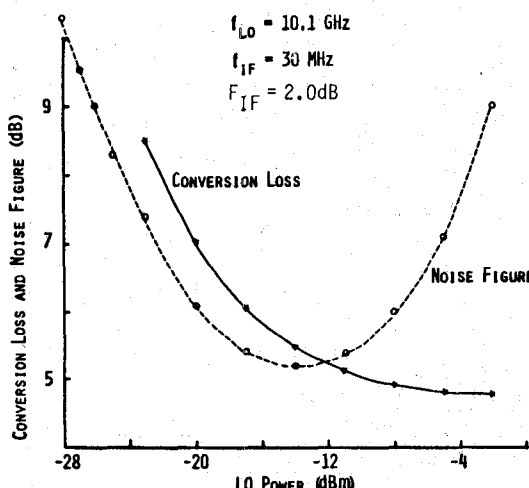


Fig. 8. Measured conversion loss and noise figure versus LO power for the X-band model mixer.

backshort reactance. Note that this match approaches the desired condition, stated earlier, that the backshort should not contribute significantly to the match.

The IF signal was amplified by means of a General Radio GR 1236 amplifier with 2-dB noise figure. The mixer noise figure was measured using a conventional HP342A noise-figure meter and 10 000 $^{\circ}$ K argon plasma noise source. Measured results of conversion loss and noise figure versus LO power shown in Fig. 8 indicate the excellent performance at low LO powers. For example, noise figures of 6.2 dB can be achieved for -20 dBm (10 μ W) of LO power and 5.2 dB for -16 dBm (24 μ W). Of interest also is that conversion loss improves with increasing LO power, while noise figure requires an optimum LO drive. At lower drive levels, noise figure is limited by deteriorating conversion loss and at higher drives may be limited by an increasing effective diode noise or by sideband noise from the LO.

Mixer RF bandwidth characteristics, obtained with a fixed backshort location, are shown in Fig. 9 for different LO drive levels. A typical 3-dB LO tuning bandwidth for -20 dBm (10 μ W) is 4.6 percent for a fixed backshort location, and over 10 percent with backshort tuning. These

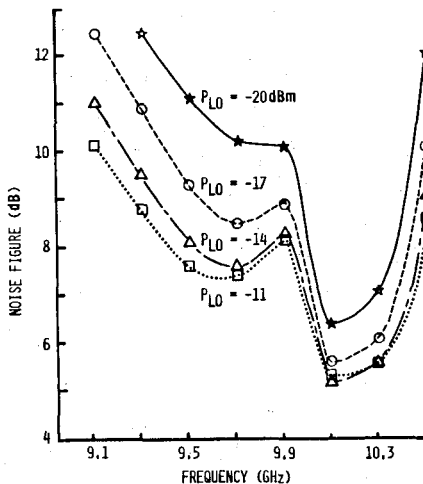


Fig. 9. Measured noise figure versus frequency for the *X*-band model mixer with fixed backshort. $F_{IF} = 2.0$ dB.

bandwidths agree with theory. Results for the *X*-band model mixer experiment verify the expected good low LO power performance and demonstrate both the effectiveness of the full-height waveguide RF matching technique and of the hybrid IC matching circuit for the IF.

VI. 235-GHz MIXER

The schematic for the 235-GHz mixer resembles that of the *X*-band model mixer of Fig. 6, except that the diode chip and whisker replace the packaged diode and pin. Circuit dimensions and diode parameters for the two mixers are compared in Table II. Both the RF choke with 52Ω and 110Ω microstrip sections and the IF matching network with hybrid planar capacitors and inductors were directly scaled from the similar circuits designed and tested for the *X*-band model. Circuit patterns consisting of $200\text{-}\text{\AA}$ titanium and $2.5\text{ }\mu\text{m}$ of gold were deposited on 0.127-mm -thick quartz substrates using standard photolithographic techniques. The diode chip, fabricated by Millimeter Wave Technology and consisting of a large array of $1\text{-}\mu\text{m}$ -diam diodes, was soldered on the RF choke. Contact to an individual diode was accomplished by means of a 0.254-mm -diam nickel gold whisker that was etched to a $1\text{-}\mu\text{m}$ tip diameter. Fig. 10 shows a photomicrograph of the whisker diode contact. The waveguide was mechanically tuned by a contacting backshort. The backshort is a U-shaped beryllium copper plunger slotted along the longitudinal dimension to assure several point contacts with the waveguide.

The mixer waveguide portion was machined from two blocks that mate asymmetrically among the broadwall dimension of the waveguide, according to a technique discussed by Kerr *et al.* [9]. In order to facilitate assembly, one block includes the capacitive post, diode assembly, RF choke, and IF and bias circuits shown in Fig. 6. The other block completes the waveguide and acts as a cover plate for the printed circuit.

Noise-figure measurements were taken using the setup shown in Fig. 11. The setup includes a mechanical chopper wheel and a 20-dB standard gain horn connected to a

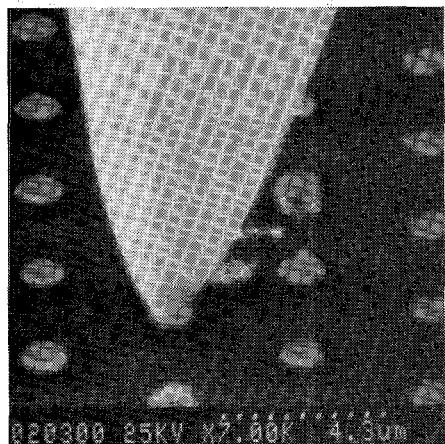


Fig. 10. Photomicrograph of the whisker diode contact.

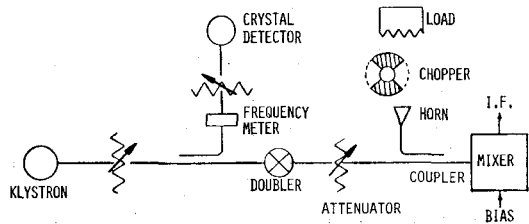


Fig. 11. Simplified RF schematic of the noise measuring setup for the 235-GHz mixer.

directional coupler at the mixer input. The chopper wheel was covered with Emerson and Cummings AN72 absorber material (except for the cut outs) and chopped at a rate of ~ 100 Hz. A hot load consisting of an infrared thermal source Infrared Industries Model 406 with a 1-in aperture cone was used. The effective temperature of this source was 970°K .³ LO power from a VRT 2123A Varian Klystron at 117.6 GHz, doubled by using a MV-38-37 Custom Microwave frequency doubler, was applied to the mixer through an attenuator and a directional coupler. The first IF amplifier was a 500–1000-MHz MITEQ AM-3A-0510 with $NF = 1.8$ dB. In order to minimize extraneous noise introduced from the chopper motor, the IF signal was translated to 30 MHz by means of another mixer. Finally, the IF signal was applied to a crystal detector and measured with an Ithaca amplifier.

A problem encountered in the measurement of the mixer characteristics was that no direct means were available for measuring power at 235 GHz. The discussion below summarizes the technique used for estimating LO power and presents measured diode characteristics and noise-figure results. Estimates of the LO power incident on the mixer diode during the noise-figure measurements were obtained from the mixer diode dc bias voltage and current as measured with and without RF drive. From a simple analysis of the mixer diode exponential I – V characteristic,

³The 970°K effective noise-source temperature was obtained from calibration measurements taken with another mixer using this source and a cold source at LN_2 (77°K) temperature. The hot source was used for this experiment in order to obtain a larger signal from the noise source.

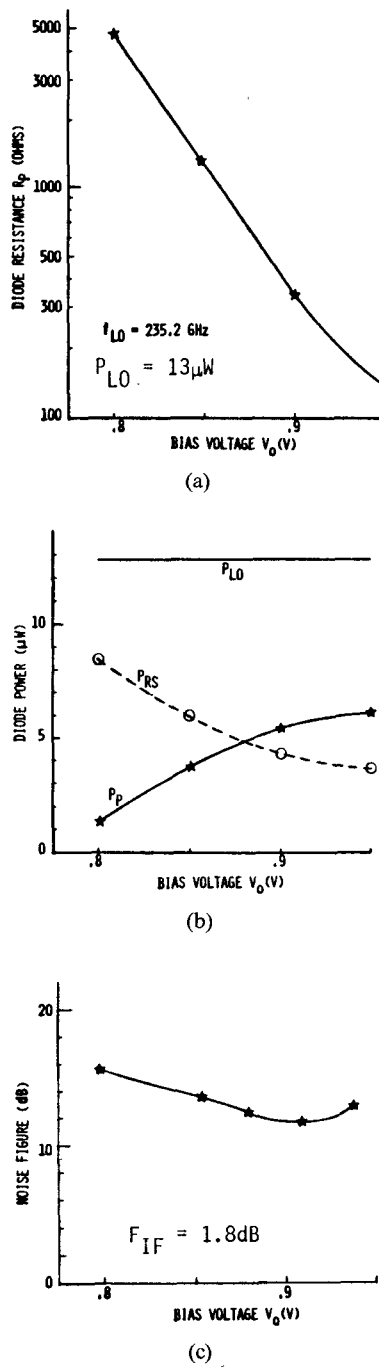


Fig. 12. (a) Measured diode resistance, (b) diode powers, and (c) double sideband noise figure versus bias voltage for the 235-GHz mixer.

one calculates [2]

$$I_0 = i_{\text{sat}} \exp(SV_0) I_1(SV_1) \quad (2)$$

$$P_{RP} = i_{\text{sat}} V_0 \exp(SV_0) I_1(SV_1) \quad (3)$$

where I_0 is the measured dc bias current, V_0 is the measured dc bias voltage, and $I_1(\cdot)$ is the modified Bessel function.

Diode parameters i_{sat} , S , and R_s were obtained from the measured diode dc characteristics. One can calculate V_1 by substituting into (2) measurements of I_0 taken at constant V_0 with and without LO power. P_{RP} is then obtained from (3) and R_p from (1). P_{LO} and C_j were obtained by

substituting into (1) values for V_1 and P_{RP} that were measured at the same LO power and at two different bias voltages. The variation of C_j with bias voltage was calculated using (A8). LO power incident on the diode was obtained from P_{LO} and the measured power reflection coefficient.

Within the accuracy of these measurements, $R_s = 14.8 \Omega$ (no LO power)⁴ and $C_j = 4 \times 10^{-15} F$ (maximum LO power) agree with the manufacturer's specifications. Because of the high insertion loss of waveguide components preceding the mixer, and probably also because of low doubler conversion efficiency, LO power incident on the mixer was limited to $\sim 13 \mu\text{W}$. Fig. 12 depicts the variation with bias voltage of diode input resistance R_p , diode powers P_{RP} , P_{RS} , and double sideband noise figure. With the maximum available LO power of $13 \mu\text{W}$, the lowest measured noise figure for $f_{LO} = 235.2$ GHz was 11.5 dB. This noise-figure measurement occurs at the same $V_0 = 0.875$ V that was calculated for lowest conversion loss. The diode to full-height waveguide match with measured power reflection coefficient $|\rho|^2 = 0.23$ was adequate and consequently was not further optimized. Based on theory, it is expected that noise figure can be improved substantially if LO power incident on the mixer can be increased from $13 \mu\text{W}$ to about $40 \mu\text{W}$.

VII. CONCLUSION

This paper has shown that single-ended whisker contacted millimeter-wave mixers can operate well at low LO powers provided that the mixer diode parasitics are low and the diode is situated in RF and IF circuits with appropriately high-embedding impedances. A capacitive post matching scheme situated in a full-height waveguide was described which is relatively easy to fabricate at short millimeter wavelengths and is suitable for high-impedance operation. Experimental results obtained on an X -band simulating model and on a 235-GHz mixer corroborate the theoretical findings.

APPENDIX

An expression for C_j , the effective junction capacitance for the diode, may be obtained as follows. The junction capacitance C_{j0} for a Schottky barrier on a uniformly doped semiconductor is given by

$$C_{j0} = C_{j0} \phi^{1/2} (\phi - V)^{-1/2} \quad (A1)$$

where

$$\phi = V_{bi} - \frac{kT}{q}$$

C_{j0} is the zero voltage junction capacitance, V_{bi} is the built-in potential, and V is the applied voltage.

The current i_c through C_{j0} is obtained from

$$\begin{aligned} i_c &= C_{j0} \frac{dV}{dt} + V \frac{dC_{j0}}{dt} \\ &= \frac{dV}{dt} \left(C_{j0} + V \frac{dC_{j0}}{dV} \right). \end{aligned} \quad (A2)$$

⁴The inclusion of skin effect in the calculations would increase R_s by about 2.5Ω [10] and decrease C_j by less than 10 percent.

The applied voltage across the diode

$$V = V_0 + V_1 \cos \omega_{LO} t \quad (A3)$$

where V_0 is the bias voltage and V_1 is the LO voltage.

Substituting (A3) and (A1) into (A2), the result is

$$i_c = -V_1 \omega_{LO} \phi^{1/2} C_{j0} \sin \omega_{LO} t \left[(\phi - V_0 - V_1 \cos \omega_{LO} t)^{-1/2} + 0.5 V_1 (\phi - V_0 - V_1 \cos \omega_{LO} t)^{-3/2} \cos \omega_{LO} t \right]. \quad (A4)$$

Average power dissipation P_{RS} by the diode resistance R_s is obtained from

$$P_{RS} = \frac{1}{2\pi} \int_0^{2\pi} i_s^2 R_s d(\omega_{LO} t) \quad (A5)$$

where $i_s = i_c + i_p$, with i_s the current through R_s and i_p the current through R_p .

For typical low LO power operation, R_p is sufficiently large to satisfy the condition that $(\omega_{LO} C_j)^2 \gg R_p^{-2}$ or that $|i_c|^2 \gg |i_p|^2$.

Thus, (A5) becomes

$$P_{RS} \approx \frac{1}{2\pi} \int_0^{2\pi} i_c^2 R_s d(\omega_{LO} t). \quad (A6)$$

By equating P_{RS} from (A6) with the expression given by (1) in the text and solving for C_j , we obtain

$$C_j = \left[\frac{\frac{1}{2\pi} \int_0^{2\pi} i_c^2 R_s d(\omega_{LO} t)}{0.5 \omega_{LO}^2 R_s V_1^2} \right]^{1/2}. \quad (A7)$$

Then substituting (A4) into (A7) the result is

$$C_j = C_{j0} \left[\frac{\phi}{\pi} \int_0^{2\pi} \sin^2 \omega_{LO} t \left[(\phi - V_0 - V_1 \cos \omega_{LO} t)^{-1/2} + 0.5 V_1 (\phi - V_0 - V_1 \cos \omega_{LO} t)^{-3/2} \cos \omega_{LO} t \right]^2 d(\omega_{LO} t) \right]^{1/2}. \quad (A8)$$

ACKNOWLEDGMENT

The author wishes to thank Dr. B. B. O'Brien for helpful discussions throughout the course of this work, and Dr. J. W. Tully for help with implementing the millimeter-wave diodes. Thanks also go to J. W. Felder for developing the mechanical design, to L. Hes for machining the 235-GHz device, and to M. D. Brown for providing the required technical report. Finally, the author wishes to thank the

reviewers for their suggestions to improve the clarity of this paper.

REFERENCES

- [1] J. W. Archer, "All solid-state low-noise receivers for 210-240 GHz," *IEEE Trans. Microwave Theory Tech.*, vol. MTT-30, pp. 1247-1252, Aug. 1982.
- [2] A. A. M. Saleh, *Theory of Resistive Mixers*, Research Monograph 64. Cambridge, MA: MIT Press, 1971.
- [3] M. McColl, "Conversion loss limitations on Schottky barrier mixers," *IEEE Trans. Microwave Theory Tech.*, vol. MTT-25, pp. 54-58, Jan. 1977.
- [4] A. R. Kerr, "Low-noise room-temperature and cryogenic mixers for 80-120 GHz," *IEEE Trans. Microwave Theory Tech.*, vol. MTT-23, pp. 781-787, Oct. 1975.
- [5] W. M. Sharpless, "Wafer type millimeter wave rectifiers," *Bell Syst. Tech. J.*, vol. 35, pp. 1385-1402, Nov. 1956.
- [6] R. L. Eisenhart and P. J. Khan, "Theoretical and experimental analysis of a waveguide mounting structure," *IEEE Trans. Microwave Theory Tech.*, vol. MTT-19, pp. 706-719, Aug. 1971.
- [7] N. Marcuvitz, *Waveguide Handbook*, (MIT Rad. Lab. Series, vol. 10). New York: McGraw-Hill, 1950.
- [8] R. DeBrecht and M. Caulton, "Lumped elements in microwave integrated circuits in the 1-12 GHz range," in *1970 IEEE G-MTT Int. Symp. Dig.*, pp. 14-16.
- [9] A. R. Kerr, R. J. Mattauch, and J. A. Grange, "A new mixer design for 140-220 GHz," *IEEE Trans. Microwave Theory Tech.*, vol. MTT-25, pp. 399-401, May 1977.
- [10] W. M. Kelly and G. T. Wrixon, "Conversion losses in Schottky-barrier diode mixers in the submillimeter region," *IEEE Trans. Microwave Theory Tech.*, vol. MTT-27, pp. 665-672, July 1979.



William Hant (S'56-M'57-SM'79) received the B.S. degree in electrical engineering from the University of California, Berkeley, in 1956, the M.S. degree from Stanford University, Stanford, CA, in 1958, and the Ph.D. degree from the University of California, Los Angeles, in 1970.

Most of his professional career has been directed toward the research and development of electron devices. From 1958 to 1970, while employed by Hughes Aircraft Company, he was involved with the development of traveling-wave tubes (TWT's). He directed programs to develop several coupled-cavity TWT amplifiers, to enhance TWT efficiency, and to investigate submillimeter-wave electron-beam harmonic generators. Since 1970, he has been associated with Northrop Corporation, where he has been engaged in the research and development of flat-panel electron-beam display devices, large area laser electron guns, and millimeter-wave solid-state components and circuits. More recently, his interests have focused on the study of high-speed integrated circuits. He has presented and published papers on microwave tubes, display devices, electron guns, and millimeter-wave components, and holds six patents in these fields.

Dr. Hant is a member of Sigma Xi, Tau Beta Pi, and Eta Kappa Nu.